PERGAMON

International Journal of Solids and Structures 39 (2002) 4787–4804

INTERNATIONAL JOURNAL OF SOLIDS and STRUCTURES

www.elsevier.com/locate/ijsolstr

Modeling of singular stress fields using finite element method

Andrzej Seweryn *

Faculty of Mechanical Engineering, Bialystok University of Technology, Wiejska 45C Street, 15-351 Białystok, Poland

Received 27 September 2001; received in revised form 29 April 2002

Abstract

The paper discusses methods of modeling of singular stress fields in problems with angular corners. A novel method of analytical constraints has been proposed. In this method the relations between the displacements of the finite element nodes are assumed to conform to the analytical solution. The method of analytical constraints has been used for calculations of the stress intensity factors and of the coefficients of the two consecutive terms of the asymptotic solution in the case of elements with cracks and V-notches under uniaxial and biaxial loading. Singular finite elements have been applied and various mesh discretisations have been used.

Keywords: Finite element method; V-notch; Stress singularity; Stress intensity factors

1. Introduction

The ability to predict fracture of structural components is of fundamental importance for reliability of any engineering design. Fracture initiation and its subsequent propagation occur in regions of high stress and strain gradients. It is therefore necessary to accurately determine the stress–strain concentrations and for this purpose various analytical, numerical and experimental methods have been developed.

Analytical methods of linear elastic fracture mechanics can be applied to problems of relatively simple geometry. Here, analysis of singular stress fields at sharp angular corners is of particular importance (see for example Williams, 1952; Parton and Perlin, 1984; Seweryn and Molski, 1996). Let us consider an infinite linear elastic plate with a V-shaped notch with a wedge angle of 2β and a system of polar coordinates (r, ϑ), with an origin at the tip of the notch (Fig. 1). The dominant singularity governing the behavior of the stresses σ_{ij} and displacements u_i in the notch-tip region has the form (Seweryn and Molski, 1996):

$$\begin{aligned} \sigma_{ij} &= \frac{K_{\mathrm{I}}^{\lambda}}{(2\pi r)^{1-\lambda_{\mathrm{I}}}} c_{ij}(\vartheta) + \frac{K_{\mathrm{II}}^{\lambda}}{(2\pi r)^{1-\lambda_{\mathrm{II}}}} d_{ij}(\vartheta), \\ u_i &= \frac{r}{2\mu}\left[\frac{K_{\mathrm{I}}^{\lambda}}{(2\pi r)^{1-\lambda_{\mathrm{I}}}} a_i(\vartheta) + \frac{K_{\mathrm{II}}^{\lambda}}{(2\pi r)^{1-\lambda_{\mathrm{II}}}} b_i(\vartheta)\right], \end{aligned} \quad (1)$$

* Tel.: +48-85-7455592; fax: +48-85-7421113.
E-mail address: seweryn@cksr.ac.bialystok.pl (A. Seweryn).

0020-7683/02/$ - see front matter
PII: S0020-7683(02)00371-2

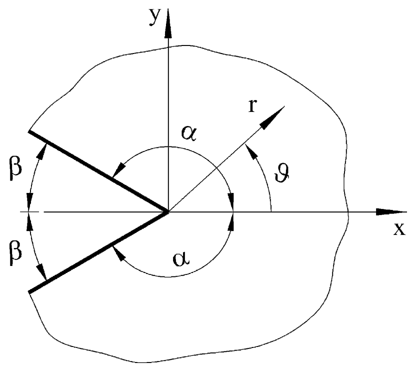

Fig. 1. Notch geometry and polar coordinates (r, ϑ).

where K_{I}^{λ} and $K_{\mathrm{II}}^{\lambda}$ are the generalized opening mode (mode I) and sliding mode (mode II) stress intensity factors (Seweryn, 1990b; Seweryn and Zwolinski, 1993), λ_{I} and λ_{II} are the exponents of the displacement field for the modes I and II, $c_{ij}(\vartheta)$, $d_{ij}(\vartheta)$, $a_i(\vartheta)$, $b_i(\vartheta)$ are trigonometric functions, μ denotes the shear modulus.

Numerical methods provide for modeling of the stress fields conforming to the analytical solution and enable evaluation of fracture mechanics parameters such as the stress intensity factors. In general the finite element method and the boundary element method are of the most practical importance (Liebowitz and Moyer, 1989; Aliabadi, 1997).

The stress singularities are modeled to conform to the analytical solution. Special singular finite elements and boundary elements have been developed to account for the appropriate singularity (see for example works by Akin, 1982; Portela et al., 1991; or Aliabadi and Rooke, 1991) and to facilitate evaluation of the generalized stress intensity factors (Babuska and Miller, 1994; Szabo and Yosibash, 1996).

Among the special finite elements the following three groups are the most commonly used:

- degenerated asymptotic finite elements (Tracey, 1971; Tracey and Cook, 1977; Pu et al., 1978);
- hybrid (or enriched) finite elements (Lin and Tong, 1980; Heyliger and Kriz, 1989);
- analytical finite elements (Givoli and Rivkin, 1993).

The main idea behind the asymptotic finite elements is to find a transformation that converts a normal finite element, such as for example a quadrilateral element with constant stress distribution or a quadrilateral element with linear stress distribution into a triangular element with the required hyperbolic singularity (see for example: Blackburn, 1972; Akin, 1976; Yamada et al., 1979).

Singular stress fields can be also modeled by using another class of finite elements known as hybrid finite elements. The formulation of the above elements combines the classical finite element approximation with the asymptotic solution in the vicinity of an angular corner (Tong et al., 1973; Tong and Pian, 1973; Benzley, 1974). Adding analytic expressions (1) to the conventional approximating polynomial yields the following displacement field within a hybrid element:

$$u_i = \sum_{j=1}^{m} N_{ij}\left[q_j - K_{\mathrm{I}}^{\lambda}\psi_i(\lambda_{\mathrm{I}}, r_j, \vartheta_j) - K_{\mathrm{II}}^{\lambda}\phi_i(\lambda_{\mathrm{II}}, r_j, \vartheta_j)\right] + K_{\mathrm{I}}^{\lambda}\psi_i(\lambda_{\mathrm{I}}, r, \vartheta) + K_{\mathrm{II}}^{\lambda}\phi_i(\lambda_{\mathrm{II}}, r, \vartheta), \tag{2}$$

where N_{ij} are standard interpolating functions, q_j are nodal displacements, r_j and ϑ_j are the coordinates of the element nodes in the polar coordinate system (r, ϑ) and functions ψ_i and ϕ_i can be obtained from (1).

The above allows for the direct calculation of the stress intensity factors. The stress intensity factors are just additional unknowns in the problem.

The idea of introducing analytical elements is based on application in the core region, around the singular point of the corner, theoretical solution for stresses and displacements with unknown constant factors, e.g. stress intensity factors (Givoli and Rivkin, 1993). The remaining area of the structure can be modeled using classic finite elements.

The powerful tool for computational fracture mechanics is the penalty-equilibrium hybrid stress element method proposed by Wu and Cheug (1995) and Xiao et al. (1999). It is an improvement on the original stress element method in that the element formulation is based on a penalty Hellinger–Reissner principle and the traction boundary conditions on a crack or notch edge are enforced exactly.

The methods of computing of the generalized stress intensity factors can be classified as follows:

- direct methods—here the values of the generalized stress intensity factors are evaluated directly as the basic unknowns in the problem (in addition to for example the nodal displacements),
- asymptotic methods—the idea is to compare the stresses or displacements obtained numerically with the analytic solution,
- energy based methods—the approach is based either on the reciprocal theorem or on the evaluation of the change of the potential energy associated with crack propagation.

The asymptotic methods of calculating the generalized stress intensity factors are based on the analytic expressions for the stress and displacement fields in the vicinity of the notch tip. Eq. (1) can be used to evaluate the stress intensity factors K_{I}^{λ} and $K_{\mathrm{II}}^{\lambda}$ at a given point with coordinates (r, ϑ) provided the stresses and displacements at that point are known from some numerical solution. As the stress intensity factors are computed at some distance r from the notch vertex extrapolation techniques have to be used in order to improve accuracy (Tracey, 1977). In accordance with the analytic solution extrapolation with respect to the coordinate $r^{1-\lambda}$ is required (Seweryn, 1990a). In another asymptotic method the stress intensity factors K_{I}^{λ} and $K_{\mathrm{II}}^{\lambda}$ are computed by evaluating the change of shape of the notch (or crack) edges in the tip vicinity (Chow and Lan, 1976; Seweryn, 1990a; He et al., 1997). The values of the displacements along the notch edges can be easily related to the values of the stress intensity factors.

In the energy based approach the mode I stress intensity factor for a crack K_{I} can be evaluated from the following relation between the total strain energy V and the strain energy release rate G_{I}:

$$G_{\mathrm{I}} = \frac{K_{\mathrm{I}}^2}{E'} = -\frac{\partial V}{\partial l} = \frac{1}{2}\frac{\partial \mathbf{q}^{\mathrm{T}}}{\partial l}\mathbf{Q} + \frac{1}{2}\mathbf{q}^{\mathrm{T}}\frac{\partial \mathbf{Q}}{\partial l} = -\frac{1}{2}\mathbf{q}^{\mathrm{T}}\frac{\partial \mathbf{K}}{\partial l}\mathbf{q} + \mathbf{q}^{\mathrm{T}}\frac{\partial \mathbf{Q}}{\partial l}, \tag{3}$$

where $E' = E$—for plane stress and $E' = E/(1-\nu^2)$—for plane strain, $\mathbf{Q}$ and $\mathbf{q}$ are the nodal force and the global displacement vectors, $\mathbf{K}$ is the stiffness matrix.

In numerical implementation of the above method (compliance method), two finite element analyses are carried out for two crack lengths l and $l + \Delta l$ with the same finite element mesh (Vaynshtok, 1977). In another energy based approach the stress intensity factor K_{I} is evaluated by displacing the crack tip node (Parks, 1974; Hellen, 1975; Nikishkov and Vaynshtok, 1980; Yang et al., 2001).

The stress intensity factor K_{I} can also be evaluated by using the crack closure integral. The above integral corresponds to the energy release rate G_{I} expressed in terms of the work of the internal forces at the tip of the crack on the opening displacement, required to extend the crack by a small distance Δl (Rybicki and Kanninen, 1977).

A common way of computing the stress intensity factor K_{I} is to use the path-independent integral J (Rice, 1968; Cherepanov, 1967). In mixed-mode problems the stress and displacement fields must be decomposed into the symmetric and anti-symmetric parts. The second approach to evaluation of the stress intensity factors $K_{\rm I}$ and $K_{\rm II}$ is based on invariant integrals J_x and J_y, that are equivalent to the components of the energy flux (Cherepanov, 1979):

$$J_x = \int_C \left(w n_x - \sigma_{ij} \frac{\partial u_i}{\partial x} n_j \right) {\rm d}s, \quad J_y = \int_C \left(w n_y - \sigma_{ij} \frac{\partial u_i}{\partial y} n_j \right) {\rm d}s, \tag{4}$$

where C is the contour of integration, $\mathbf{n}(n_1, n_2)$ is the unit vector normal to C, ds is an infinitesimal increment of arc length along C and w is the strain energy density.

The generalized stress intensity factors can also be determined using methods based on Betti's reciprocal theorem (Stern and Soni, 1976; Sinclair et al., 1984; Carpenter, 1984; Labossiere and Dunn, 1998). The factor $K_{\rm I}^{\lambda}$ can be determined by evaluating the integral along the contour Γ (around the notch tip) and using stresses σ_{ij} and displacements u_i obtained from the finite element solution, namely:

$$K_{\rm I}^{\lambda} = H_{\rm I} = \int_{\Gamma} (\sigma_{ij} u_i^* - \sigma_{ij}^* u_i) n_j \, {\rm d}s. \tag{5}$$

The complementary stresses σ_{ij}^* and displacements u_i^* are determined from integral (5), based on the analytic expressions (1) for the stress and displacement fields in the vicinity of the notch tip. Similar relations can be derived for the case of a V-notch subjected to mode II loading (anti-symmetric problem).

2. Method of analytical constraints

Analysis of fracture of structural elements with cracks or sharp corners subjected to complex loading conditions requires accurate evaluation of the generalized stress intensity factors $K_{\rm I}^{\lambda}$ and $K_{\rm II}^{\lambda}$. In the paper by Ramulu and Kobayashi (1994) and Seweryn (1998) it has been demonstrated that under certain loading conditions it is necessary to consider the higher order terms of the asymptotic expansion. Among the methods mentioned in the previous section just the method of hybrid elements (or analytical elements) enables inclusion of the higher order terms. In this section an alternative and simpler method of analytical constraints is presented.

The method of analytical constraints combined with the finite element method can be effectively applied to problems with angular corners for direct and accurate calculation of the stress intensity factors as well as the coefficients of the higher order terms in the asymptotic expansion of the stress field. Contrary to for example the asymptotic methods in the method of analytical constraints one assumes that the displacements of the finite element nodes conform to the analytic solution rather than just using the nodal displacements obtained from a numerical solution for calculation of other parameters.

The idea of the method is described below using an example problem of fracture mechanics. Let us consider a body with a crack as illustrated in Fig. 2. The region is covered with a finite element mesh with m nodes. The displacements of the finite element nodes in the region around the crack tip $\Omega_{\rm A}$ are constrained by the analytic relations. The remaining part of the body is referred to as the region $\Omega_{\rm O}$. The region $\Omega_{\rm O}$ contains $n-1$ nodes (numbered from 1 through $n-1$) with unaltered degrees of freedom (nodal displacements). The region $\Omega_{\rm A}$ contains $m-n+1$ nodes (numbered from n through m), for which the initial number of degrees of freedom has been reduced from $2(m-n+1)$ to k (as there are $2(m-n+1)$ analytic relations with k parameters).

The global displacement vector $\mathbf{q}$ is divided into two parts (subvectors):

- vector of displacement components of nodes with analytical constraints (region $\Omega_{\rm A}$)—$\mathbf{u}_{\rm A} = \{u_n, v_n, u_{n+1}, v_{n+1}, \ldots, u_m, v_m\}$,
- vector of displacement components of all other nodes (region $\Omega_{\rm O}$)—$\mathbf{u}_{\rm O} = \{u_1, v_1, \ldots, u_{n-1}, v_{n-1}\}$, that is

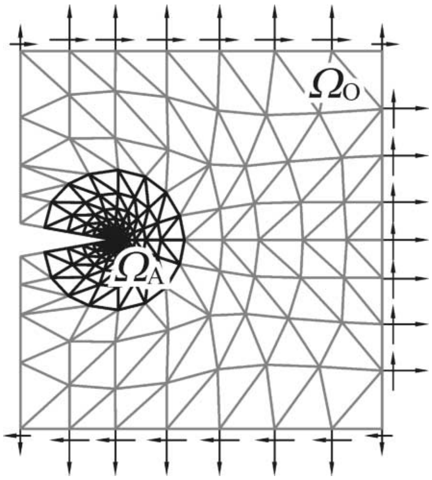

Fig. 2. Body containing a crack and regions Ω_A and Ω_O.

$$\mathbf{q}^T = \{\mathbf{u}_O^T, \mathbf{u}_A^T\}. \tag{6}$$

The strain energy of the system can be written as

$$U = \frac{1}{2}\mathbf{q}^T\mathbf{K}\mathbf{q} = \frac{1}{2}\{\mathbf{u}_O^T, \mathbf{u}_A^T\}\begin{bmatrix} \mathbf{K}_{OO} & \mathbf{K}_{AO} \\ \mathbf{K}_{OA} & \mathbf{K}_{AA} \end{bmatrix}\begin{Bmatrix} \mathbf{u}_O \\ \mathbf{u}_A \end{Bmatrix}, \tag{7}$$

where $\mathbf{K}$ is the global stiffness matrix.

Let us consider the singular stress and displacement distributions in the crack tip region given by

$$\begin{aligned} \sigma_{ij} &= \frac{1}{\sqrt{2\pi r}}\left[K_I f_{ij}^I(\vartheta) + K_{II} f_{ij}^{II}(\vartheta)\right], \\ u_i &= \frac{r}{2\mu\sqrt{2\pi r}}\left[K_I g_i^I(\vartheta) + K_{II} g_i^{II}(\vartheta)\right] + u_{Ci}, \end{aligned} \tag{8}$$

where (r, ϑ) are polar coordinates with an origin at the crack tip, K_I and K_{II} denotes the mode I and mode II stress intensity factors, u_{Ci} are displacement components of the crack (or notch) tip.

Let us introduce a modified vector of nodal parameters:

$$\mathbf{q}^{*T} = \{\mathbf{u}_O^T, \mathbf{u}_K^T\}, \tag{9}$$

where $\mathbf{u}_K$ is the vector of analytical parameters containing less components than the vector $\mathbf{u}_A$. For the considered crack problem as expressed by (8) the above vector takes the form:

$$\mathbf{u}_K^T = \{K_I, K_{II}, u_C, v_C\}. \tag{10}$$

The relationship between $\mathbf{q}$ and $\mathbf{q}^*$ can be written as follows:

$$\mathbf{q} = \mathbf{G}\mathbf{q}^*, \tag{11}$$

or

$$\begin{Bmatrix} \mathbf{u}_O \\ \mathbf{u}_A \end{Bmatrix} = \begin{bmatrix} \mathbf{I} & 0 \\ 0 & \mathbf{\Psi} \end{bmatrix}\begin{Bmatrix} \mathbf{u}_O \\ \mathbf{u}_K \end{Bmatrix},$$

where $\mathbf{I}$ is unit matrix and $\mathbf{\Psi}$ is the matrix of analytical constraints.

The matrix of analytical constraints $\boldsymbol{\Psi}$ relates the degrees of freedom (nodal displacements in region Ω_A) to analytical parameters (i.e. the stress intensity factors K_I and K_{II} and the displacement components at the crack tip u_C and v_C), namely:

$$\mathbf{u}_A = \boldsymbol{\Psi}\mathbf{u}_K. \tag{12}$$

Assuming that analytical constraints have been imposed on nodes with indexes from n to m and using relations (8) the matrix of analytical constraints $\boldsymbol{\Psi}$ becomes:

$$\boldsymbol{\Psi} = \frac{1}{2\mu\sqrt{2\pi}}\begin{bmatrix} \sqrt{r_n}g_1^{I}(\vartheta_n) & \sqrt{r_n}g_1^{II}(\vartheta_n) & 2\mu\sqrt{2\pi} & 0 \\ \sqrt{r_n}g_2^{I}(\vartheta_n) & \sqrt{r_n}g_2^{II}(\vartheta_n) & 0 & 2\mu\sqrt{2\pi} \\ \sqrt{r_{n+1}}g_1^{I}(\vartheta_{n+1}) & \sqrt{r_{n+1}}g_1^{II}(\vartheta_{n+1}) & 2\mu\sqrt{2\pi} & 0 \\ \cdots & \cdots & \cdots & \cdots \\ \sqrt{r_m}g_2^{I}(\vartheta_m) & \sqrt{r_m}g_2^{II}(\vartheta_m) & 0 & 2\mu\sqrt{2\pi} \end{bmatrix}, \tag{13}$$

where r_n, ϑ_n stand for coordinates of the node with an index n in the polar coordinate system with an origin at the crack tip.

Substituting (11) into (7) the strain energy of the system U can be written as follows:

$$U = \tfrac{1}{2}\mathbf{q}^{*T}(\mathbf{G}^T\mathbf{K}\mathbf{G})\mathbf{q}^* = \tfrac{1}{2}\mathbf{q}^{*T}\mathbf{K}^*\mathbf{q}^*, \tag{14}$$

where $\mathbf{K}^*$ denotes the modified stiffness matrix:

$$\mathbf{K}^* = \begin{bmatrix} \mathbf{K}_{OO} & \mathbf{K}_{AO}\boldsymbol{\Psi} \\ \boldsymbol{\Psi}^T\mathbf{K}_{OA} & \boldsymbol{\Psi}^T\mathbf{K}_{AA}\boldsymbol{\Psi} \end{bmatrix}. \tag{15}$$

Simple modification of the global stiffness matrix should be carried out while composing the local stiffness matrixes. The boundary conditions of the problem can be taken into consideration following a similar procedure. The load vector $\mathbf{Q}$ should be modified as follows:

$$\mathbf{Q}^* = \mathbf{G}^T\mathbf{Q}. \tag{16}$$

The above relation results from the following expression for the work of external forces W:

$$W = \mathbf{q}^T\mathbf{Q} = \mathbf{q}^{*T}(\mathbf{G}^T\mathbf{Q}). \tag{17}$$

Let us consider the stress and displacement distributions at the crack tip given by the following expansions (Williams, 1957):

$$\begin{aligned} \sigma_{ij} &= \sum_{k=1}^{m_1} K_{Ik} r^{(k/2)-1} f_{ij}^{Ik}(\vartheta) + \sum_{k=1}^{m_2} K_{IIk} r^{(k/2)-1} f_{ij}^{IIk}(\vartheta), \\ u_i &= \sum_{k=1}^{m_1} K_{Ik} r^{k/2} g_i^{Ik}(\vartheta) + \sum_{k=1}^{m_2} K_{IIk} r^{k/2} g_i^{IIk}(\vartheta) + u_{Ci}, \end{aligned} \tag{18}$$

where m_1 and m_2 are the numbers of terms in the solution for mode I and II, respectively. It should be noted, that $K_{I1} = K_I$ and $K_{II1} = K_{II}$ and the term $K_{II2}\ r g_i^{II2}(\vartheta)$ corresponds to rigid rotation of the crack tip region (and the local coordinate system).

The vector of analytical parameters becomes:

$$\mathbf{u}_K^T = \{K_I, K_{I2}, K_{I3}, \ldots, K_{Im_1}, K_{II}, K_{II2}, K_{II3}, \ldots, K_{IIm_2}, u_C, v_C\}, \tag{19}$$

and the matrix of analytical constraints imposed on nodes from n to m can be written as follows:

$$\boldsymbol{\Psi} = \begin{bmatrix} \sqrt{r_n}g_1^{\mathrm{I1}}(\vartheta_n) & r_n g_1^{\mathrm{I2}}(\vartheta_n) & r_n^{3/2}g_1^{\mathrm{I3}}(\vartheta_n) & \cdots & \sqrt{r_n}g_1^{\mathrm{II1}}(\vartheta_n) & r_n g_1^{\mathrm{II2}}(\vartheta_n) & r_n^{3/2}g_1^{\mathrm{II3}}(\vartheta_n) & \cdots & 1 & 0 \\ \sqrt{r_n}g_2^{\mathrm{I1}}(\vartheta_n) & r_n g_2^{\mathrm{I2}}(\vartheta_n) & r_n^{3/2}g_2^{\mathrm{I3}}(\vartheta_n) & \cdots & \sqrt{r_n}g_2^{\mathrm{II1}}(\vartheta_n) & r_n g_2^{\mathrm{II2}}(\vartheta_n) & r_n^{3/2}g_2^{\mathrm{II3}}(\vartheta_n) & \cdots & 0 & 1 \\ \sqrt{r_{n+1}}g_1^{\mathrm{I1}}(\vartheta_{n+1}) & r_{n+1} g_1^{\mathrm{I2}}(\vartheta_{n+1}) & r_{n+1}^{3/2}g_1^{\mathrm{I3}}(\vartheta_{n+1}) & \cdots & \sqrt{r_{n+1}}g_1^{\mathrm{II1}}(\vartheta_{n+1}) & r_{n+1} g_1^{\mathrm{II2}}(\vartheta_{n+1}) & r_{n+1}^{3/2}g_1^{\mathrm{II3}}(\vartheta_{n+1}) & \cdots & 1 & 0 \\ \cdots & \cdots & \cdots & \cdots & \cdots & \cdots & \cdots & \cdots & \cdots & \cdots \\ \sqrt{r_m}g_2^{\mathrm{I1}}(\vartheta_m) & r_m g_2^{\mathrm{I2}}(\vartheta_m) & r_m^{3/2}g_1^{\mathrm{I3}}(\vartheta_m) & \cdots & \sqrt{r_m}g_2^{\mathrm{II1}}(\vartheta_m) & r_m g_2^{\mathrm{II2}}(\vartheta_m) & r_m^{3/2}g_1^{\mathrm{II3}}(\vartheta_m) & \cdots & 0 & 1 \end{bmatrix}. \tag{20}$$

For angular corners the matrix of analytical constraints $\boldsymbol{\Psi}$ can be derived using the asymptotic series solutions for the stress and displacement fields:

$$\begin{aligned} \sigma_{ij} &= \sum_{k=1}^{m_1} K_{\mathrm{I}k}^{\lambda} r^{\lambda_{\mathrm{I}k}-1} f_{ij}^{\mathrm{I}}(\vartheta, \lambda_{\mathrm{I}k}) + \sum_{k=1}^{m_2} K_{\mathrm{II}k}^{\lambda} r^{\lambda_{\mathrm{II}k}-1} f_{ij}^{\mathrm{II}}(\vartheta, \lambda_{\mathrm{II}k}), \\ u_i &= \sum_{k=1}^{m_1} K_{\mathrm{I}k}^{\lambda} r^{\lambda_{\mathrm{I}k}} g_i^{\mathrm{I}}(\vartheta, \lambda_{\mathrm{I}k}) + \sum_{k=1}^{m_2} K_{\mathrm{II}k}^{\lambda} r^{\lambda_{\mathrm{II}k}} g_i^{\mathrm{II}}(\vartheta, \lambda_{\mathrm{II}k}) + u_{\mathrm{C}i}, \end{aligned} \tag{21}$$

where $\lambda_{\mathrm{I}k}$ and $\lambda_{\mathrm{I}k}$ are consecutive solutions of the characteristic equation for the opening and shearing modes, $K_{\mathrm{I1}}^{\lambda} = K_{\mathrm{I}}^{\lambda}$, $K_{\mathrm{II}k}^{\lambda} = K_{\mathrm{II}}^{\lambda}$ are the generalized stress intensity factors, defined by the relations:

$$K_{\mathrm{I}}^{\lambda} + \mathrm{i}K_{\mathrm{II}}^{\lambda} = \lim_{\vartheta=0\, r\to 0}[(2\pi r)^{1-\lambda_{\mathrm{I}}}\sigma_{\vartheta\vartheta}(r,\vartheta) + \mathrm{i}(2\pi r)^{1-\lambda_{\mathrm{II}}}\tau_{r\vartheta}(r,\vartheta)]. \tag{22}$$

The vector of analytical parameters takes the form

$$\mathbf{u}_{\mathrm{K}}^{\mathrm{T}} = \{K_{\mathrm{I}}^{\lambda}, K_{\mathrm{I2}}^{\lambda}, K_{\mathrm{I3}}^{\lambda}, \ldots, K_{\mathrm{I}m_1}^{\lambda}, K_{\mathrm{II}}^{\lambda}, K_{\mathrm{II2}}^{\lambda}, K_{\mathrm{II3}}^{\lambda}, \ldots, K_{\mathrm{I}m_2}^{\lambda}, u_{\mathrm{C}}, v_{\mathrm{C}}\}, \tag{23}$$

and the matrix of analytical constraints becomes:

$$\boldsymbol{\Psi} = \begin{bmatrix} r_n^{\lambda_{\mathrm{I1}}} g_1^{\mathrm{I}}(\vartheta_n, \lambda_{\mathrm{I1}}) & \cdots & r_n^{\lambda_{\mathrm{I}m1}} g_1^{\mathrm{I}}(\vartheta_n, \lambda_{\mathrm{I}m1}) & r_n^{\lambda_{\mathrm{II1}}} g_1^{\mathrm{II}}(\vartheta_n, \lambda_{\mathrm{II1}}) & \cdots & r_n^{\lambda_{\mathrm{II}m2}} g_1^{\mathrm{II}}(\vartheta_n, \lambda_{\mathrm{II}m2}) & 1 & 0 \\ r_n^{\lambda_{\mathrm{I1}}} g_2^{\mathrm{I}}(\vartheta_n, \lambda_{\mathrm{I1}}) & \cdots & r_n^{\lambda_{\mathrm{I}m1}} g_2^{\mathrm{I}}(\vartheta_n, \lambda_{\mathrm{I}m1}) & r_n^{\lambda_{\mathrm{II1}}} g_2^{\mathrm{II}}(\vartheta_n, \lambda_{\mathrm{II1}}) & \cdots & r_n^{\lambda_{\mathrm{II}m2}} g_2^{\mathrm{II}}(\vartheta_n, \lambda_{\mathrm{II}m2}) & 0 & 1 \\ r_{n+1}^{\lambda_{\mathrm{I1}}} g_1^{\mathrm{I}}(\vartheta_{n+1}, \lambda_{\mathrm{I1}}) & \cdots & r_{n+1}^{\lambda_{\mathrm{I}m1}} g_1^{\mathrm{I}}(\vartheta_{n+1}, \lambda_{\mathrm{I}m1}) & r_{n+1}^{\lambda_{\mathrm{II1}}} g_1^{\mathrm{II}}(\vartheta_{n+1}, \lambda_{\mathrm{II1}}) & \cdots & r_{n+1}^{\lambda_{\mathrm{II}m2}} g_1^{\mathrm{II}}(\vartheta_{n+1}, \lambda_{\mathrm{II}m2}) & 1 & 0 \\ \cdots & \cdots & \cdots & \cdots & \cdots & \cdots & \cdots & \cdots \\ r_m^{\lambda_{\mathrm{I1}}} g_1^{\mathrm{I}}(\vartheta_m, \lambda_{\mathrm{I1}}) & \cdots & r_m^{\lambda_{\mathrm{I}m1}} g_1^{\mathrm{I}}(\vartheta_m, \lambda_{\mathrm{I}m1}) & r_m^{\lambda_{\mathrm{II1}}} g_1^{\mathrm{II}}(\vartheta_m, \lambda_{\mathrm{II1}}) & \cdots & r_m^{\lambda_{\mathrm{II}m2}} g_1^{\mathrm{II}}(\vartheta_m, \lambda_{\mathrm{II}m2}) & 1 & 0 \\ r_m^{\lambda_{\mathrm{I1}}} g_2^{\mathrm{I}}(\vartheta_m, \lambda_{\mathrm{I1}}) & \cdots & r_m^{\lambda_{\mathrm{I}m1}} g_2^{\mathrm{I}}(\vartheta_m, \lambda_{\mathrm{I}m1}) & r_m^{\lambda_{\mathrm{II1}}} g_2^{\mathrm{II}}(\vartheta_m, \lambda_{\mathrm{II1}}) & \cdots & r_m^{\lambda_{\mathrm{II}m2}} g_1^{\mathrm{II}}(\vartheta_m, \lambda_{\mathrm{II}m2}) & 0 & 1 \end{bmatrix}. \tag{24}$$

If the exponent of the kth term of the asymptotic expansion is complex ($\lambda_k = \mathrm{Re}\,\lambda_k + \mathrm{i}\mathrm{Im}\,\lambda_k, \mathrm{Im}\,\lambda_k \neq 0$), then also the conjugate value $\overline{\lambda}_k = \mathrm{Re}\,\lambda_k - \mathrm{i}\mathrm{Im}\,\lambda_k$, satisfies the problem conditions. The stress intensity factor K_k^{λ} is also complex ($K_k^{\lambda} = \mathrm{Re}K_k^{\lambda} + \mathrm{i}\mathrm{Im}K_k^{\lambda}$) and its conjugate ($\overline{K}_k^{\lambda} = \mathrm{Re}K_k^{\lambda} - \mathrm{i}\mathrm{Im}K_k^{\lambda}$) corresponds to the conjugate of the exponent λ_k. Thus, a complex term in the asymptotic expansion implies two analytical parameters $\mathrm{Re}K_k^{\lambda}$ and $\mathrm{Im}K_k^{\lambda}$. The stress and displacement distributions are given by

$$\begin{aligned} \sigma_{ij} &= \sum_{k=1}^{m_1} \left\{ \mathrm{Re}K_{\mathrm{I}k}^{\lambda}\mathrm{Re}\left[r^{\lambda_{\mathrm{I}k}-1} f_{ij}^{\mathrm{I}}(\vartheta, \lambda_{\mathrm{I}k})\right] - \mathrm{Im}K_{\mathrm{I}k}^{\lambda}\mathrm{Im}\left[r^{\lambda_{\mathrm{I}k}-1} f_{ij}^{\mathrm{I}}(\vartheta, \lambda_{\mathrm{I}k})\right]\right\} \\ &\quad + \sum_{k=1}^{m_2} \left\{ \mathrm{Re}K_{\mathrm{II}k}^{\lambda}\mathrm{Re}\left[r^{\lambda_{\mathrm{II}k}-1} f_{ij}^{\mathrm{II}}(\vartheta, \lambda_{\mathrm{II}k})\right] - \mathrm{Im}K_{\mathrm{II}k}^{\lambda}\mathrm{Im}\left[r^{\lambda_{\mathrm{II}k}-1} f_{ij}^{\mathrm{II}}(\vartheta, \lambda_{\mathrm{II}k})\right]\right\}, \\ u_i &= \sum_{k=1}^{m_1} \left\{ \mathrm{Re}K_{\mathrm{I}k}^{\lambda}\mathrm{Re}\left[r^{\lambda_{\mathrm{I}k}} g_i^{\mathrm{I}}(\vartheta, \lambda_{\mathrm{I}k})\right] - \mathrm{Im}K_{\mathrm{I}k}^{\lambda}\mathrm{Im}\left[r^{\lambda_{\mathrm{I}k}} g_i^{\mathrm{I}}(\vartheta, \lambda_{\mathrm{I}k})\right]\right\} \\ &\quad + \sum_{k=1}^{m_2} \left\{ \mathrm{Re}K_{\mathrm{II}k}^{\lambda}\mathrm{Re}\left[r^{\lambda_{\mathrm{II}k}} g_i^{\mathrm{II}}(\vartheta, \lambda_{\mathrm{II}k})\right] - \mathrm{Im}K_{\mathrm{II}k}^{\lambda}\mathrm{Im}\left[r^{\lambda_{\mathrm{II}k}-1} g_i^{\mathrm{II}}(\vartheta, \lambda_{\mathrm{II}k})\right]\right\}. \end{aligned} \tag{25}$$

The vector of analytical parameters takes the form:

$$\mathbf{u}_{\mathrm{K}}^{\mathrm{T}} = \{\mathrm{Re}\,K_{\mathrm{I}1}^{\lambda}, \mathrm{Im}\,K_{\mathrm{I}1}^{\lambda}, \mathrm{Re}\,K_{\mathrm{I}2}^{\lambda}, \ldots, \mathrm{Re}\,K_{\mathrm{I}m_1}^{\lambda}, \mathrm{Im}\,K_{\mathrm{I}m_1}^{\lambda}, \mathrm{Re}\,K_{\mathrm{II}1}^{\lambda}, \mathrm{Im}\,K_{\mathrm{II}1}^{\lambda}, \mathrm{Re}\,K_{\mathrm{II}2}^{\lambda}, \ldots, \mathrm{Re}\,K_{\mathrm{I}m_2}^{\lambda}, \mathrm{Im}\,K_{\mathrm{I}m_2}^{\lambda}, u_{\mathrm{C}}, v_{\mathrm{C}}\}. \tag{26}$$

Of course, if $\mathrm{Im}\,\lambda_{\mathrm{I}k} = 0$ or $\mathrm{Im}\,\lambda_{\mathrm{II}k} = 0$, then one should skip the corresponding analytical parameter $\mathrm{Im}\,K_{\mathrm{I}k}^{\lambda}$ or $\mathrm{Im}\,K_{\mathrm{II}k}^{\lambda}$ in the above vector.The matrix of analytical constraints becomes:

$$\boldsymbol{\Psi} = \begin{bmatrix} \mathrm{Re}\big[r_n^{\lambda_{\mathrm{I}1}} g_1^{\mathrm{I}}(\vartheta_n, \lambda_{\mathrm{I}1})\big] & \mathrm{Im}\big[r_n^{\lambda_{\mathrm{I}1}} g_1^{\mathrm{I}}(\vartheta_n, \lambda_{\mathrm{I}1})\big] & \mathrm{Re}\big[r_n^{\lambda_{\mathrm{I}2}} g_1^{\mathrm{I}}(\vartheta_n, \lambda_{\mathrm{I}2})\big] & \ldots & \mathrm{Im}\big[r_n^{\lambda_{\mathrm{II}m2}} g_1^{\mathrm{II}}(\vartheta_n, \lambda_{\mathrm{II}m2})\big] & 1 & 0 \\ \mathrm{Re}\big[r_n^{\lambda_{\mathrm{I}1}} g_2^{\mathrm{I}}(\vartheta_n, \lambda_{\mathrm{I}1})\big] & \mathrm{Im}\big[r_n^{\lambda_{\mathrm{I}1}} g_2^{\mathrm{I}}(\vartheta_n, \lambda_{\mathrm{I}1})\big] & \mathrm{Re}\big[r_n^{\lambda_{\mathrm{I}2}} g_2^{\mathrm{I}}(\vartheta_n, \lambda_{\mathrm{I}2})\big] & \ldots & \mathrm{Im}\big[r_n^{\lambda_{\mathrm{II}m2}} g_2^{\mathrm{II}}(\vartheta_n, \lambda_{\mathrm{II}m2})\big] & 0 & 1 \\ \mathrm{Re}\big[r_{n+1}^{\lambda_{\mathrm{I}1}} g_1^{\mathrm{I}}(\vartheta_{n+1}, \lambda_{\mathrm{I}1})\big] & \mathrm{Im}\big[r_{n+1}^{\lambda_{\mathrm{I}1}} g_1^{\mathrm{I}}(\vartheta_{n+1}, \lambda_{\mathrm{I}1})\big] & \mathrm{Re}\big[r_{n+1}^{\lambda_{\mathrm{I}2}} g_1^{\mathrm{I}}(\vartheta_{n+1}, \lambda_{\mathrm{I}2})\big] & \ldots & \mathrm{Im}\big[r_{n+1}^{\lambda_{\mathrm{II}m2}} g_1^{\mathrm{II}}(\vartheta_{n+1}, \lambda_{\mathrm{II}m2})\big] & 1 & 0 \\ \ldots & \ldots & \ldots & \ldots & \ldots & \ldots & \ldots \\ \mathrm{Re}\big[r_m^{\lambda_{\mathrm{I}1}} g_1^{\mathrm{I}}(\vartheta_m, \lambda_{\mathrm{I}1})\big] & \mathrm{Im}\big[r_m^{\lambda_{\mathrm{I}1}} g_1^{\mathrm{I}}(\vartheta_m, \lambda_{\mathrm{I}1})\big] & \mathrm{Re}\big[r_m^{\lambda_{\mathrm{I}2}} g_1^{\mathrm{I}}(\vartheta_m, \lambda_{\mathrm{I}2})\big] & \ldots & \mathrm{Im}\big[r_m^{\lambda_{\mathrm{II}m2}} g_1^{\mathrm{II}}(\vartheta_m, \lambda_{\mathrm{II}m2})\big] & 1 & 0 \\ \mathrm{Re}\big[r_m^{\lambda_{\mathrm{I}1}} g_2^{\mathrm{I}}(\vartheta_m, \lambda_{\mathrm{I}1})\big] & \mathrm{Im}\big[r_m^{\lambda_{\mathrm{I}1}} g_2^{\mathrm{I}}(\vartheta_m, \lambda_{\mathrm{I}1})\big] & \mathrm{Re}\big[r_m^{\lambda_{\mathrm{I}2}} g_2^{\mathrm{I}}(\vartheta_m, \lambda_{\mathrm{I}2})\big] & \ldots & \mathrm{Im}\big[r_m^{\lambda_{\mathrm{II}m2}} g_2^{\mathrm{II}}(\vartheta_m, \lambda_{\mathrm{II}m2})\big] & 0 & 1 \end{bmatrix}. \tag{27}$$

It should be pointed out that one can hardly find any physical interpretation for the complex terms with $0 < \mathrm{Re}\,\lambda < 1$. The resulting singular stress field is oscillating with the frequency of the sign changes increasing infinitely towards the vertex of an angular corner. Such a solution is also obtained for a crack along the interface of two materials as well as for an angular corner with one edge free and the other clamped.

One should note that in the method of analytical constraints the displacement field is continuous across the element boundaries. On the other hand, in the method of hybrid elements displacement discontinuities occur along the boundaries between the hybrid and the standard finite elements. To overcome the above problem one has to introduce special interface elements (see for example Benzley, 1974).

It is important to note that analytical elements method and constraint method are conceptually similar. The difference lays in details. In the first case theoretical solution is imposed directly (for example as function of constant analytical factors), but in the other the known character of the solution is approximated using shape functions of the finite elements. Thus, in the later case it is necessary to use asymptotic finite elements.

3. Results of computations of stress intensity factors

3.1. Sheet with a central crack subjected to tensile and shear loading

The numerical methods presented in the previous sections have been applied to evaluate the stress intensity factors and the coefficients of leading terms in the asymptotic expansion of the stress field near the notch tip. A square sheet with dimensions $b = h = 10$ and with a central crack of length $2l = 2$ (Fig. 3) has been analyzed. The following four loading cases have been considered:

(a) tensile loading in the direction perpendicular to the crack plane $\sigma_2 = 100$;
(b) tensile loading in the direction parallel to the crack plane $\sigma_1 = 100$;
(c) biaxial tensile loading ($\sigma_1 = \sigma_2 = 100$);
(d) shear loading $\tau = 100$.

Let us take into consideration the first, the second and the third terms of the asymptotic expansion of the stress field at the crack tip. The components of the stress tensor and displacement vector are written as

- for mode I loading:

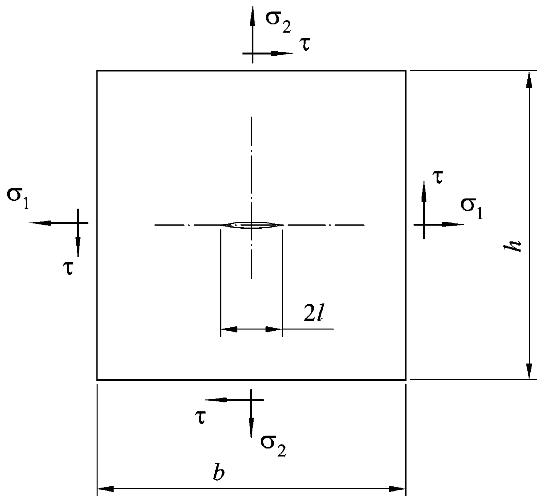

Fig. 3. Sheet containing a central crack subjected to tensile and shear loading.

$$
\begin{aligned}
\sigma_{rr} &= \frac{K_{I1}}{4\sqrt{2\pi r}}\left(5\cos\frac{\vartheta}{2} - \cos\frac{3}{2}\vartheta\right) - K_{I2}\cos^2\vartheta + \frac{K_{I3}}{4}\sqrt{2\pi r}\left(3\cos\frac{\vartheta}{2} + \cos\frac{5\vartheta}{2}\right),\\
\sigma_{\vartheta\vartheta} &= \frac{K_{I1}}{4\sqrt{2\pi r}}\left(3\cos\frac{\vartheta}{2} + \cos\frac{3}{2}\vartheta\right) - K_{I2}\sin^2\vartheta + \frac{K_{I3}}{4}\sqrt{2\pi r}\left(5\cos\frac{\vartheta}{2} - \cos\frac{5\vartheta}{2}\right),\\
\tau_{r\vartheta} &= \frac{K_{I1}}{4\sqrt{2\pi r}}\left(\sin\frac{\vartheta}{2} + \sin\frac{3}{2}\vartheta\right) + K_{I2}\sin\vartheta\cos\vartheta + \frac{K_{I3}}{4}\sqrt{2\pi r}\left(\sin\frac{\vartheta}{2} - \sin\frac{5\vartheta}{2}\right),\\
u_r &= \frac{K_{I1}}{2\mu}\sqrt{\frac{r}{2\pi}}\cos\frac{\vartheta}{2}(\kappa - \cos\vartheta) - \frac{K_{I2}r}{8\mu}(\kappa - 1 + \cos 2\vartheta) + \frac{K_{I3}r}{12\mu}\sqrt{2\pi r}\left((2\kappa-3)\cos\frac{\vartheta}{2} + \cos\frac{5\vartheta}{2}\right),\\
u_\vartheta &= \frac{-K_{I1}}{2\mu}\sqrt{\frac{r}{2\pi}}\sin\frac{\vartheta}{2}(\kappa - \cos\vartheta) + \frac{K_{I2}r}{4\mu}\sin 2\vartheta + \frac{K_{I3}r}{12\mu}\sqrt{2\pi r}\left((2\kappa+3)\sin\frac{\vartheta}{2} - \sin\frac{5\vartheta}{2}\right),
\end{aligned}
\tag{28}
$$

- for mode II loading:

$$
\begin{aligned}
\sigma_{rr} &= \frac{-K_{II1}}{4\sqrt{2\pi r}}\left(5\sin\frac{\vartheta}{2} - 3\sin\frac{3\vartheta}{2}\right) + \frac{K_{II3}}{4}\sqrt{2\pi r}\left(3\sin\frac{\vartheta}{2} + 5\sin\frac{5\vartheta}{2}\right),\\
\sigma_{\vartheta\vartheta} &= \frac{-3K_{II1}}{4\sqrt{2\pi r}}\left(\sin\frac{\vartheta}{2} + 3\sin\frac{3\vartheta}{2}\right) + \frac{K_{II3}}{4}\sqrt{2\pi r}\left(5\sin\frac{\vartheta}{2} - 5\sin\frac{5\vartheta}{2}\right),\\
\tau_{r\vartheta} &= \frac{K_{II1}}{4\sqrt{2\pi r}}\left(\cos\frac{\vartheta}{2} + 3\cos\frac{3\vartheta}{2}\right) - \frac{K_{II3}}{4}\sqrt{2\pi r}\left(5\cos\frac{\vartheta}{2} - 5\cos\frac{5\vartheta}{2}\right),\\
u_r &= \frac{K_{II1}}{2\mu}\sqrt{\frac{r}{2\pi}}\sin\frac{\vartheta}{2}(2 - \kappa + 3\cos\vartheta) + \frac{K_{II3}r}{12\mu}\sqrt{2\pi r}\left((2\kappa-3)\sin\frac{\vartheta}{2} + 5\sin\frac{5\vartheta}{2}\right),\\
u_\vartheta &= \frac{-K_{II1}}{2\mu}\sqrt{\frac{r}{2\pi}}\cos\frac{\vartheta}{2}(2 + \kappa - 3\cos\vartheta) + K_{II2}r - \frac{K_{II3}r}{12\mu}\sqrt{2\pi r}\left((2\kappa+3)\cos\frac{\vartheta}{2} - 5\cos\frac{5\vartheta}{2}\right),
\end{aligned}
\tag{29}
$$

where r, ϑ are polar coordinates with an origin at the crack tip.

$$\kappa = \begin{cases} (3-\nu)/(1+\nu) & \text{for plane stress,} \\ (3-4\nu) & \text{for plane strain,} \end{cases}$$

ν is Poisson's ratio.

It should be pointed out, that the coefficients of the dominant singular terms in expressions (28) and (29) are just the classic stress intensity factors $K_{\text{I}1} = K_{\text{I}}$ and $K_{\text{II}1} = K_{\text{II}}$. The second term of the solution for the sliding mode describes rotation of the system with respect to the crack tip. The second term for the opening mode characterizes the normal compression stresses along the crack plane. It should be noted, that for the case (b) the problem is nonsingular and can be described just by the second term of the asymptotic solution.

Due to the double symmetry (in cases (a), (b) and (c)) and anti-symmetry (in case (d)) only the upper right quarter of the sheet has been modeled. Two basic finite element discretisations have been used:

(1) mesh containing 112 elements (251 nodes) with node number 251 located at the tip;
(2) mesh containing 160 elements (353 nodes) with node number 353 located at the tip.

Both cases have been illustrated in Fig. 4, the basic difference being the mesh density in the tip region (8 elements surrounding the tip in the first case as shown Fig. 4b have been replaced by 56 elements in the second case as shown in Fig. 4c).

Two types of finite elements were used:

- special 6-node triangular asymptotic finite elements AST (Seweryn, 1990c; Seweryn et al., 1997) used in some cases for the first row of elements surrounding the crack tip (8 elements);
- standard 6-node triangular finite elements of the second order used for the whole mesh or for the whole mesh except the elements surrounding the crack tip.

The analytical constraints were imposed on the displacements of the nodes in the tip vicinity. There are 50 constraints if one assumes the analytic solution in the nodes of the first row of elements (27 nodes give 54 degrees of freedom and there are three boundary conditions and one displacement component of the tip node remains unknown). Similarly there will be 116 constraints if the analytic solution is assumed in the nodes of the first two rows of elements etc. The elements of the constraint matrix have been computed considering from one to three leading terms of the asymptotic solution. According to literature for the loading cases (a) and (c) the stress intensity factor is $K_{\text{I}} = 187.8$ (Bowie and Neal, 1970) and obviously for the loading case (b) one has $K_{\text{I}1} = 0$ and $K_{\text{I}2} = -100$. The results of calculations are given in Tables 1–3.

Accuracy of the results is quite high. In a number of cases the stress intensity factors K_{I} and K_{II} as well as coefficient $K_{\text{I}2}$ were computed with an error below 1%.

It should be pointed out that increasing the mesh density had only a limited effect on the accuracy. The number of terms of asymptotic expansion taken into consideration seems to be a more significant factor. In order to achieve a reasonable accuracy it is necessary to incorporate two or for some cases even three terms but further increase of the number of terms does not influence the results of computations of K_{I} and K_{II}. If standard finite elements are used for the whole mesh (including the crack tip vicinity) the error gets about 5%. The above error can be reduced by increasing the mesh density and by imposing analytical constraints over a larger region surrounding the crack tip (in comparison to the mesh with special finite elements in the crack tip vicinity).

3.2. Sheet containing an angled central crack

As another example the problem of a square sheet with an angled central crack under tension was solved (Fig. 5). The sheet dimensions were assumed to be $b = h = 10$, the crack length was $2l = 2$, the crack

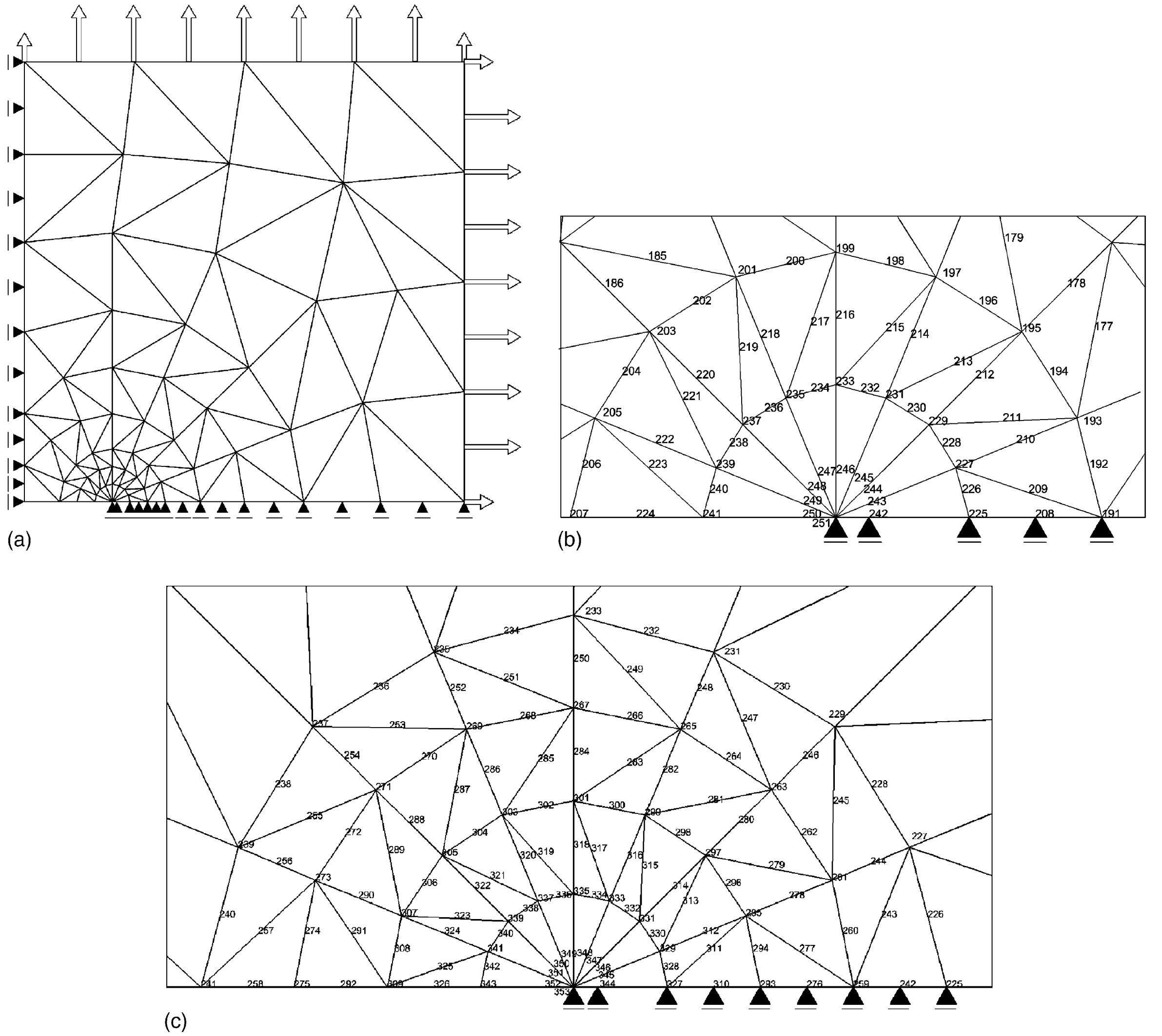

Fig. 4. (a) The finite element mesh for a sheet with a central crack; (b, c) crack tip region for the mesh containing respectively 112 and 160 elements.

Table 1
Computed values of the coefficients K for the sheet with a central crack subjected to tensile loading (opening mode: mode I)

Number of terms in solution	Number of analytical constraints	$\sigma_1 = 0$, $\sigma_2 = 100$			$\sigma_1 = 100$, $\sigma_2 = 100$			$\sigma_1 = 100$, $\sigma_2 = 0$		
		K_I	K_{I2}	K_{I3}	K_I	K_{I2}	K_{I3}	K_I	K_{I2}	K_{I3}
1	50	169.5	–	–	182.3	–	–	12.73	–	–
2	50	180.8	90.862	–	181.2	−8.6	–	0.455	−99.49	–
3	50	186.7	106.41	21.9	187.2	6.95	21.94	0.46	−99.47	0.035
1	116	157.5	–	–	178.1	–	–	20.68	–	–
2	116	174.4	83.401	–	174.9	−16.17	–	0.443	−99.56	–
3	116	185.8	104.55	21.8	186.2	5.01	21.86	0.470	−99.51	0.055

Total number of elements—112, number of singular elements—8.

Table 2
Computed values of the coefficients K for the sheet with a central crack subjected to tensile loading (opening mode: mode I)

Number of terms in solution	Number of analytical constraints	$\sigma_1 = 0$, $\sigma_2 = 100$			$\sigma_1 = 100$, $\sigma_2 = 100$			$\sigma_1 = 100$, $\sigma_2 = 0$		
		K_I	K_{I2}	K_{I3}	K_I	K_{I2}	K_{I3}	K_I	K_{I2}	K_{I3}
2	50	185.09	98.65	–	185.56	−0.85	–	0.47	−99.50	–
3	50	186.78	107.48	24.53	187.25	7.98	24.54	0.47	−99.50	0.012
2	116	183.49	95.61	–	183.46	−3.91	–	0.46	−99.52	–
3	116	186.54	107.21	22.87	187.00	7.72	22.9	0.46	−99.49	0.039
2	182	181.84	92.85	–	182.30	−6.67	–	0.46	−99.52	–
3	182	186.40	106.89	22.68	186.86	7.40	22.70	0.46	−99.49	0.041
2	248	180.14	90.68	–	181.59	−8.85	–	0.45	−99.53	–
3	248	186.19	106.49	22.36	186.65	7.00	22.40	0.46	−99.49	0.023

Total number of elements—160, number of singular elements—8.

Table 3
Computed values of the coefficients K for the sheet with a central crack subjected to shear loading (sliding mode: mode II, $\tau = 100$)

Number of terms in solution	Number of analytical constraints	With singular finite elements			Without singular finite elements		
		K_{II}	K_{II2}	K_{II3}	K_{II}	K_{II2}	K_{II3}
2	50	183.28	32.02	–	166.37	22.36	–
3	50	183.93	35.95	21.82	166.79	25.10	15.39
2	116	182.11	28.50	–	173.09	21.08	–
3	116	183.42	34.11	21.91	174.23	26.14	20.01
2	182	181.33	30.40	–	175.16	25.51	–
3	182	183.25	37.16	21.80	176.34	31.98	20.92
2	248	180.34	26.83	–	176.07	26.38	–
3	248	183.23	34.53	21.86	178.35	33.88	21.38

Total number of elements—160.

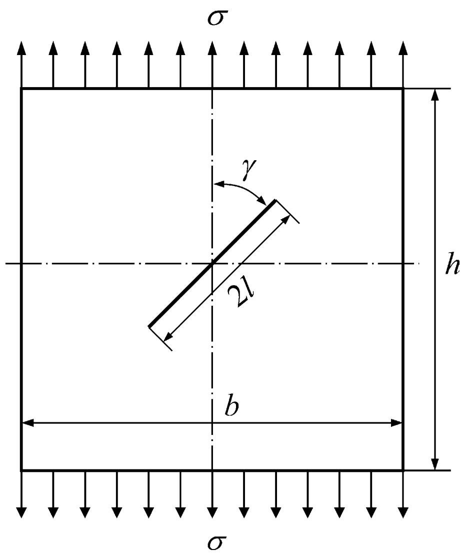

Fig. 5. Sheet containing an angled crack subjected to tension.

inclination to the direction of loading was defined by angle γ and the loading was $\sigma = 100$. The sheet was divided into 360 finite elements (Fig. 6), the crack tip being surrounded by the singular AST elements. The stress intensity factors K_I and K_{II} computed with the method of analytical constraints were compared to the values obtained using the J-integral and the H-integral. The analytical constraints were imposed on the nodes belonging to the elements surrounding the crack tip and the external boundary of that region was taken as the contour of integration of the J-integral and the H-integral. Three terms of the asymptotic expansion were taken into account for both tensile and shear loading (Eqs. (28) and (29)).

The results of calculations of the stress intensity factors K_I and K_{II} and coefficient: K_{I2}, K_{II2}, K_{I3} and K_{II3} are presented in Table 4. There is a good agreement between the values of K_I and K_{II} obtained using the method of analytical constraints and the J-integral calculations both for simple loading (Mode I or Mode II) and for complex loading (combined Modes I and II). The computations based on the invariant integrals such as the J-integral and the H-integral can provide just the values of K_I and K_{II}. The significance of the coefficient K_{I2} (that corresponds to the stress component tangent to the crack axis—see Eq. (28)) has been demonstrated by Ramulu and Kobayashi (1994) and Seweryn (1998). For cracks inclined at a small angle to

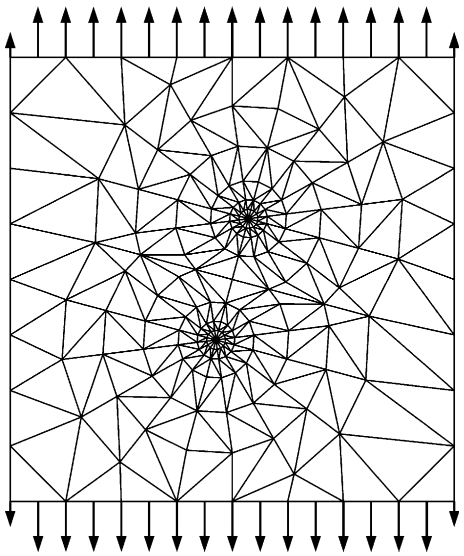

Fig. 6. The finite element mesh for a sheet with an angled crack.

Table 4
Computed values of the analytical parameters for the sheet with an angled crack

Crack angle γ (deg)	Method of analytical constrains						Contour integral J		Contour integral H	
	K_I	K_{II}	K_{I2}	K_{II2}	K_{I3}	K_{II3}	K_I	K_{II}	K_I	K_{II}
0	0.53	4e − 4	−99.28	3e − 7	0.048	2e − 4	0.314	5e − 4	0.484	2e − 4
15	12.81	45.55	−85.84	0.0156	1.55	5.42	13.09	44.92	13.23	41.60
30	46.48	79.07	−48.37	0.027	5.73	9.42	46.83	78.01	46.70	72.01
45	92.68	91.65	2.65	0.0315	11.21	10.89	92.99	90.483	92.96	83.70
60	139.25	79.61	54.07	0.027	16.76	9.46	139.66	78.64	140.10	72.47
75	173.45	46.04	92.06	0.016	20.93	5.46	173.85	45.34	174.34	42.03
90	185.95	−6e − 6	105.97	3e − 8	22.46	−3e − 4	186.34	8e − 4	186.56	6e − 4

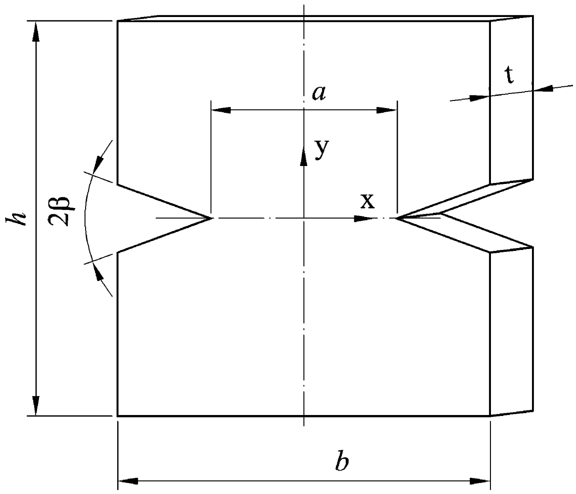

Fig. 7. The specimen with V-notches.

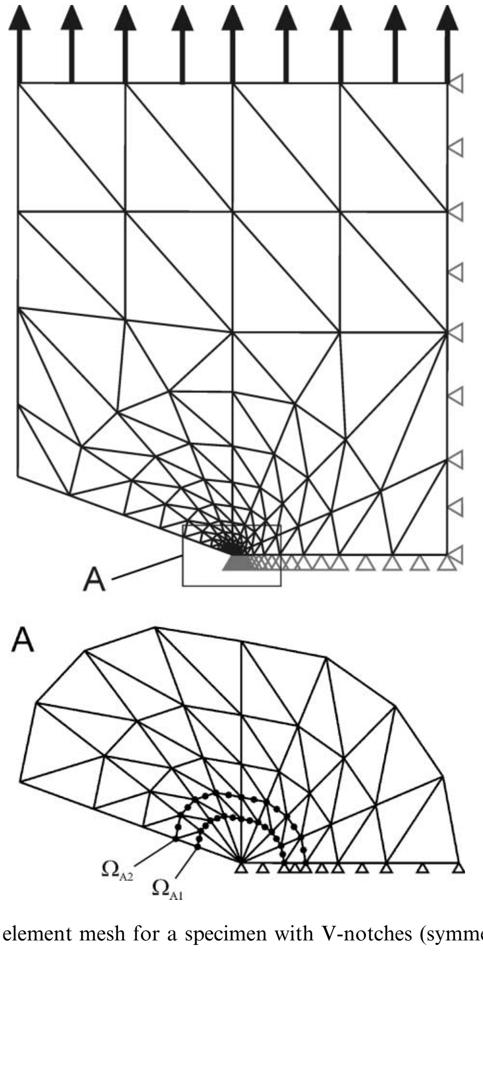

Fig. 8. The finite element mesh for a specimen with V-notches (symmetrical problem).

the direction of tension the value of K_{I2} is a major factor influencing the critical load as well as the direction of crack propagation.

3.3. Sheet with V-notches subjected to tensile and shear loading

The method of analytical constraints was used to compute the generalized stress intensity factors in the case of elements with V-notches made out of polymethyl metacrylate (PMMA) under tensile and shear loading. The problem geometry, material parameters (the Young modulus $E = 3300$ MPa, the Poisson ratio $\nu = 0.35$), boundary conditions and loads are the same as in previous experimental investigations (cf. Seweryn et al., 1997). The specimens dimensions were as follows (Fig. 7): length $h = 106$ mm, width $b = 100$ mm, the distance between notch tips $a = 50$ mm, thickness $t = 5$ mm and the wedge notch angle was varied from $2\beta = 20°$ to $2\beta = 80°$. The enforced displacements were prescribed along the upper specimen edge in the direction of y axis for tension and x axis for shear. A typical mesh of finite elements is presented in Fig. 8.

In calculations by the method of analytical constraints 2 or 3 terms of asymptotic expansions were used. The exponents of the displacement field corresponding to the terms of analytic solution are given in Table 5. Two series of computations were conducted. In the first one the analytical constraints were imposed within the finite elements directly surrounding the crack tip (region Ω_{A1}). In the second series of computations the analytical constraints were additionally imposed over the second row of elements in the crack tip vicinity (region Ω_{A2}).

The calculation results of the generalized stress intensity factors K_I^λ and K_{II}^λ referred to the values of normal and shear load components for wedge-notched specimens of the notch opening angle 2β are presented in Table 6. The tensile and shearing load components P and T have been calculated by integrating the resulting stresses across the specimen width. The results of calculations by using analytical constraint method (FEM) and H-integral method (BEM) (presented in the paper by Seweryn and Łukaszewicz (2002)) are compared.

Table 5
Value of the exponents of the displacement fields λ_{Ik} and λ_{IIk} (for mode I and II)

Notch angle 2β (deg)	Exponents λ_{Ik} (for opening)			Exponents λ_{IIk} (for sliding)		
	$k = 1$	$k = 2$	$k = 3$	$k = 1$	$k = 2$	$k = 3$
20	0.5004	1.1254	1.4976	0.5620	1.0	1.6752
40	0.5035	1.3027	1.4670	0.6382	1.0	1.9497 + 0.1265i
60	0.5122	1.4710 + 0.1418i	2.6776 + 0.2849i	0.7309	1.0	2.0749 + 0.2294i
80	0.5304	1.5724 + 0.2095i	2.8664 + 0.3493i	0.8434	1.0	2.2200 + 0.2927i

Table 6
Value of the generalized stress intensity factors for the specimens with V-notches

Notch angle 2β (deg)	Method of analytical constrains (FEM)				H-integral method (BEM) (Seweryn and Łukaszewicz, 2002)	
	Region Ω_{A1}		Region Ω_{A2}			
	K_I^λ/P	K_{II}^λ/T	K_I^λ/P	K_{II}^λ/T	K_I^λ/P	K_{II}^λ/T
20	0.6319	0.6875	0.6304	0.6867	0.6166	0.6737
40	0.6475	0.9811	0.6460	0.9854	0.6323	0.9981
60	0.6876	1.4764	0.6854	1.4930	0.6676	1.4772
80	0.7588	2.2331	0.7561	2.2869	0.7350	2.3112

4. Conclusions

The method of analytical constraints integrates the ideas of the method of the reduced basis and the method of hybrid elements. In order to conform to some analytic relations constraining the displacements the problem is formulated in terms of certain theoretical parameters (such as the stress intensity factors) instead of the displacement components. The number of the nodes where the displacements are constrained by analytic relations depends on the assumption concerning the size of the region with the theoretical solution.

Applying the method of analytical constraints reduces the number of degrees of freedom and thus reduces the time of computations (in comparison to the initial finite element mesh). The values of the analytical parameters are evaluated in a direct way from the set of equations following from minimization of the total strain energy of the system under consideration. The method can be used for the problems involving cracks and V-notches as well as any other problems where the character of the displacement field is known from theory (as for example in problems with sharp inclusions, problems with hyperbolic notches and contact problems). The accuracy of solution increases with increasing number of terms of asymptotic expansion taken into consideration. It should be emphasized that an increased accuracy of computing of field quantities by increasing the number of terms in asymptotic expansion will imply an increase of accuracy of fracture predictions provided the above terms are also incorporated into the formulation of the fracture criterion.

The method of analytical constraints enables accurate evaluation of the values of the generalized stress intensity factors and other analytical parameters even for coarse finite element meshes and does not necessarily require using special asymptotic finite elements. If standard finite elements are to be used for the whole model one should assure adequately finer mesh in the region where singularity dominates. The number of terms of the analytic solution taken into consideration should be related to the extend of the area with nodes where the analytical constraints are applied, that is for larger area more terms should be considered.

The size of the region with analytic solution can be related to the size of the damage region occurring in nonlocal fracture criteria (cf. Seweryn and Mróz, 1995, 1998).

A serious deficiency of the method of analytical constraints, similarly to the method of hybrid elements, is the need to use specialized finite element software. However, it is quite straightforward to incorporate the method of analytical constraints into the standard finite element code.

Acknowledgements

The investigation described in this paper is a part of the research project no. W/WM/1/00 sponsored by the Polish State Committee for Scientific Research and realized in Białystok University of Technology.

References

Akin, J.E., 1976. The generation of elements with singularities. Int. J. Numer. Meth. Eng. 10, 1249–1259.
Akin, J.E., 1982. Application and implementation of finite element method. Academic Press, London.
Aliabadi, M.H., 1997. Boundary element formulations in fracture mechanics. Appl. Mech. Rev. 50, 83–96.
Aliabadi, M.H., Rooke, D.P., 1991. Numerical Fracture Mechanics. Computational Mech. Publ, Southampton.
Babuska, I., Miller, A., 1994. The post-processing approach in the finite element method—Part 2: The calculation of stress intensity factors. Int. J. Numer. Meth. Eng. 20, 1111–1129.
Benzley, S.E., 1974. Representation of singularities with isoparametric finite elements. Int. J. Numer. Meth. Eng. 8, 537–545.

Blackburn, W.S., 1972. Calculation of stress intensity factors at crack tip using special finite elements. In: Whiteman, J.R. (Ed.), The Mathematics of Finite Elements and Applications. Academic Press, London, pp. 327–336.

Bowie, O.L., Neal, D.M., 1970. A note on the central crack in a uniformly stressed strip. Eng. Fract. Mech. 2 (2), 181–182.

Carpenter, W.C., 1984. Calculation of fracture parameters for a general corner. Int. J. Fract. 24, 45–58.

Cherepanov, G.P., 1967. The propagation of cracks in a continuous medium. J. Appl. Math. Mech. 31, 503–512.

Cherepanov, G.P., 1979. Mechanics of Brittle Fracture. McGraw-Hill, New York.

Chow, C.L., Lan, K.J., 1976. On crack surface displacement approaches of finite element analysis in evaluating stress intensity factors. Int. J. Fract. 12, 488–490.

Givoli, D., Rivkin, L., 1993. The DtN finite element method for elastic domains with cracks and reentrant corners. Comput. Struct. 49, 633–642.

He, W.J., Lin, Y., Ding, H.J., 1997. A three-dimensional formula for determining stress intensity factors in finite element analysis of cracked bodies. Eng. Fract. Mech. 56, 409–415.

Hellen, T.K., 1975. On the method of virtual crack extensions. Int. J. Numer. Meth. Eng. 9, 187–207.

Heyliger, P.R., Kriz, R.D., 1989. Stress intensity factors by enriched mixed finite elements. Int. J. Numer. Meth. Eng. 28, 1461–1473.

Labossiere, P.E.W., Dunn, M.L., 1998. Calculation of stress intensities at sharp notches in anisotropic media. Eng. Fract. Mech. 61, 635–654.

Liebowitz, H., Moyer Jr., E.T., 1989. Finite element methods in fracture mechanics. Comput. Struct. 31, 1–9.

Lin, K.Y., Tong, P., 1980. Singular finite elements for the fracture analysis of V-notched plate. Int. J. Numer. Meth. Eng. 15, 1343–1354.

Nikishkov, G.P., Vaynshtok, W.A., 1980. Application of the virtual crack extension method for evaluation of stress intensity factors K_I and K_{II}. Problems of Strength (6), 26–30 (in Russian).

Parks, D.M., 1974. A stiffness derivative finite element technique for determination of elastic crack tip stress intensity factor. Int. J. Fract. 10, 487–502.

Parton, V.Z., Perlin, P.I., 1984. Mathematical Methods of the Theory of Elasticity. Mir Publishers, Moscow.

Portela, A., Aliabadi, M.H., Rooke, D.P., 1991. Efficient boundary element analysis of sharp notched plates. Int. J. Numer. Meth. Eng. 32, 445–458.

Pu, S.L., Hussain, M.A., Lorensen, W.E., 1978. The collapsed cubic isoparametric element as a singular element for crack problems. Int. J. Numer. Meth. Eng. 12, 1727–1742.

Ramulu, M., Kobayashi, A.S., 1994. Numerical and experimental study of mixed mode fatigue crack propagation. In: Carpinteri, A. (Ed.), Handbook of Fatigue Crack Propagation in Metallic Structures, pp. 1073–1123.

Rice, J.L., 1968. A path independent integral and the approximate analysis of strain concentration by notches and cracks. Trans. ASME, J. Appl. Mech. 35, 379–386.

Rybicki, E.F., Kanninen, M.F., 1977. A finite element calculation of stress intensity factors by a modified crack closure integral. Eng. Fract. Mech. 9, 931–938.

Seweryn, A., 1990a. Asymptotic methods of evaluation of stress intensity factors for V-notches in plane problems of elasticity. Eng. Trans. 38, 467–486 (in Polish).

Seweryn, A., 1990b. Modeling of stress and displacement distributions near the vertex of a V-notch in plane problems of elasticity (part I). Eng. Trans. 38, 351–376 (in Polish).

Seweryn, A., 1990c. Modeling of stress and displacement distributions near the vertex of a V-notch in plane problems of elasticity (part II). Eng. Trans. 38, 377–396 (in Polish).

Seweryn, A., 1998. A non-local stress and strain energy release rate mixed mode fracture initiation and propagation criteria. Eng. Fract. Mech. 59, 737–760.

Seweryn, A., Łukaszewicz, A., 2002. Verification of brittle fracture criteria for elements with V-shaped notches. Eng. Fract. Mech. 69, 1487–1510.

Seweryn, A., Molski, K., 1996. Elastic stress singularities and corresponding generalized stress intensity factors for angular corners under various boundary conditions. Eng. Fract. Mech. 55, 529–556.

Seweryn, A., Mróz, Z., 1995. A non-local stress failure condition for structural elements under multiaxial loading. Eng. Fract. Mech. 51, 955–973.

Seweryn, A., Mróz, Z., 1998. On the criterion of damage evolution for variable multiaxial stress state. Int. J. Solids Struct. 35, 1599–1616.

Seweryn, A., Poskrobko, S., Mróz, Z., 1997. Brittle fracture in plane elements with sharp notches under mixed-mode loading. J. Eng. Mech. ASCE 123, 535–543.

Seweryn, A., Zwolinski, J., 1993. Solution for the stress and displacement fields in the vicinity of a V-notch of negative wedge angle in plane problems of elasticity. Eng. Fract. Mech. 44, 275–281.

Sinclair, G.B., Okajima, M., Griffin, J.H., 1984. Path independent integrals for computing stress intensity factors at sharp notches in elastic plates. Int. J. Numer. Meth. Eng. 20, 999–1008.

Stern, M., Soni, M.L., 1976. On the computation of stress intensities at fixed-free corners. Int. J. Solid Struct. 12, 331–337.

Szabo, B., Yosibash, Z., 1996. Numerical analysis of singularities in two-dimensions—Part 2: Computation of generalized flux/stress intensity factors. Int. J. Numer. Meth. Eng. 39, 409–434.
Tong, P., Pian, T.H.H., 1973. On the convergence of the FEM for problems with singularity. Int. J. Solid Struct. 9, 313–323.
Tong, P., Pian, T.H.H., Lasry, S.J., 1973. A hybryd-element approach to crack problems in plane elasticity. Int. J. Numer. Meth. Eng. 7, 297–308.
Tracey, D.M., 1971. Finite elements for determination of crack tip elastic stress intensity factors. Eng. Fract. Mech. 3, 255–266.
Tracey, D.M., 1977. Discussion of "On the use of isoparametric finite element in linear fracture mechanics by R.S. Barsoum". Int. J. Numer. Meth. Eng. 11, 401–402.
Tracey, D.M., Cook, T.S., 1977. Analysis of power type singularities using finite elements. Int. J. Numer. Meth. Eng. 11, 1225–1233.
Vaynshtok, W.A., 1977. Comparison of two numerical methods of calculating of stress intensity factors. Problems of Strength (9), 80–82 (in Russian).
Williams, M.L., 1952. Stress singularities resulting from various boundary conditions in angular corners of plates in extension. Trans. ASME, J. Appl. Mech. 19, 526–528.
Williams, M.L., 1957. On the stress distribution at the base of stationary crack. Trans. ASME, J. Appl. Mech. 24, 109–114.
Wu, C.C., Cheug, Y.K., 1995. On optimization approaches of hybrid stress elements. Finite Elements Anal. Des. 21, 11–28.
Xiao, Q.Z., Karihaloo, B.L., Williams, F.W., 1999. Application of penalty-equilibrium hybrid stress element method to crack problems. Eng. Fract. Mech. 63, 1–22.
Yamada, Y., Ezawa, Y., Nishiguchi, I., Okabe, M., 1979. Reconsiderations on singularity or crack tip elements. Int. J. Numer. Meth. Eng. 14, 1525–1544.
Yang, Z.J., Chen, J.F., Holt, G.D., 2001. Efficient evaluation of stress intensity factors using virtual crack extension technique. Comput. Struct. 79, 2705–2715.